Journal of Solid State Chemistry 227 (2015) 1–4

Contents lists available at ScienceDirect

Journal of Solid State Chemistry

journal homepage: www.elsevier.com/locate/jssc

Structure and magnetism of $Sr_3NiSb_2O_9$

Peter D. Battle*, Chun-Mann Chin, Sophie I. Evers, Mark Westwood

Inorganic Chemistry Laboratory, University of Oxford, South Parks Road, Oxford OX1 3QR, UK

ARTICLE INFO

Article history:
Received 12 February 2015
Received in revised form
18 March 2015
Accepted 19 March 2015
Available online 27 March 2015

Keywords:
Perovskite
Magnetic susceptibility
Neutron diffraction

ABSTRACT

The crystal structure of the perovskite-related oxide $Sr_3NiSb_2O_9$ has been refined from X-ray and neutron powder diffraction data; space group $P2_1/n$, $a=5.64381(2)$, $b=5.62299(2)$, $c=7.95687(3)$ Å, $\beta=90.014(2)^\circ$. The structure has two crystallographically-distinct six-coordinate cation sites with occupancies Sb 0.97(1), Ni 0.03 and Sb 0.36, Ni 0.64. The magnetic susceptibility has been measured over the temperature range $2 \le T/K \le 300$. Fitting data recorded in the temperature range $150 < T/K < 300$ to the Curie–Weiss law resulted in $\mu_{eff}=3.49(1)\,\mu_B$ per Ni^{2+}, $\theta=-138(1)$ K. Ferrimagnetic coupling in the vicinity of the antisite defects is suggested to be responsible for the enhanced susceptibility observed below ~90 K. The zero-field cooled susceptibility shows a maximum at 8.7 K that is not observed in the field-cooled susceptibility. Hysteresis is observed in M(H) at 2 K but not at 7.5 K.

1. Introduction

The magnetic properties of $La_3Ni_2SbO_9$, first discussed by Alvarez et al. [1], have recently been discussed in more depth by ourselves [2,3] and others [4,5]. The compound adopts a distorted perovskite structure containing two crystallographically-distinct, six-coordinate sites in an alternating 1:1 arrangement, see Fig. 1. The Ni^{2+} and Sb^{5+} cations, present in a 2:1 ratio, are distributed over these two sites such that one site is occupied only by Ni^{2+} while the other is occupied by Sb^{5+} and Ni^{2+} in a 2:1 ratio. SQUID magnetometry revealed a magnetic transition at 105 K and a magnetisation of 1.5 μ_B per formula unit was measured at 5 K in a field of 40 kOe. In order to interpret these data it was proposed that the Ni^{2+} cations on neighbouring sites couple antiferromagnetically, but the imbalance in Ni^{2+} numbers on the two sites results in a net magnetisation. However, our first neutron diffraction measurements [2] failed to identify any magnetic Bragg scattering below the transition temperature. Subsequent measurements at low temperatures identified very weak magnetic scattering, the intensity of which increased towards the expected level when a magnetic field was applied to the compound [3]. In order to account for this observation we proposed that cation disorder and variations in composition within the crystallites cause the formation of small ferrimagnetic domains whose magnetisation vectors are not aligned until a magnetic field is applied; electron microscopy has provided direct evidence of the variations in composition. By analogy with the field of ferroelectricity, we described $La_3Ni_2SbO_9$ as a relaxor ferromagnet.

$La_3Ni_2SbO_9$ can be considered to be the $x=3$ member of the system $Sr_{3-x}La_xNi_{1+x/3}Sb_{2-x/3}O_9$, where $0 \le x \le 3$. The magnetic properties of this system will clearly depend on the concentration of the magnetic Ni^{2+} cation and the composition $x=1.5$, more conveniently formulated as $SrLaNiSbO_6$, has previously been shown to be a Type I antiferromagnet at 1.7 K [6]. In view of the current interest in the Ni/Sb system we have now undertaken a study of the $x=0$ end-member $Sr_3NiSb_2O_9$. We are not the first to carry out such a study but the results described below differ from and expand on those reported previously [7].

2. Experimental

A polycrystalline sample of $Sr_3NiSb_2O_9$ was prepared by heating a stoichiometric, pelletised mixture of strontium carbonate, antimony(V) oxide and nickel oxide at 1250 °C in an alumina crucible for a total of eight days; the reaction mixture was ground and repelletised every two days. The reaction was deemed to be complete when the X-ray powder diffraction pattern of the product, recorded at room temperature using a PANalytical X'Pert Pro diffractometer operating in Bragg-Brentano geometry, did not change on further heating. Neutron diffraction data were collected at room temperature on the powder diffractometer D2b at ILL, Grenoble using a wavelength of 1.594 Å. The sample was contained in a vanadium can. Analysis of both the X-ray and neutron diffraction patterns was performed using the Rietveld [8] method as implemented in the GSAS program suite [9]. The background and peak shape were modelled using a 12-term Chebyschev

* Corresponding author.
E-mail address: peter.battle@chem.ox.ac.uk (P.D. Battle).

http://dx.doi.org/10.1016/j.jssc.2015.03.022
0022-4596/

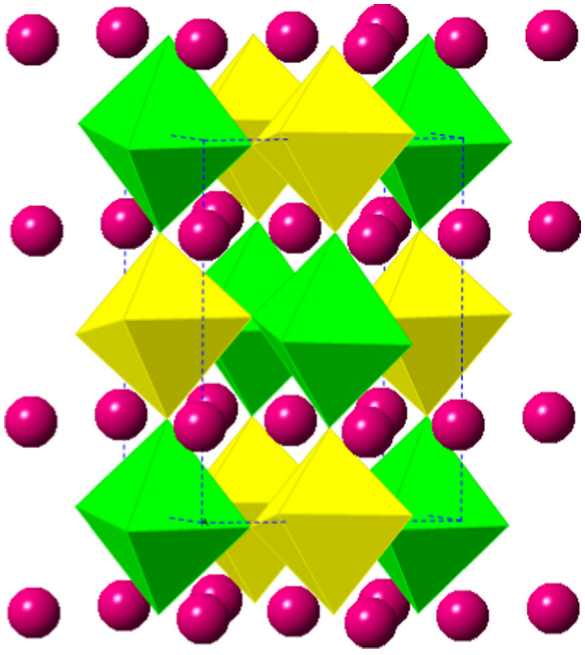

Fig. 1. Crystal structure of $Sr_{3-x}La_xNi_{1+x/3}Sb_{2-x/3}O_9$. Green and yellow octahedra represent the 2*d* and 2*c* sites respectively; purple circles represent Sr^{2+}/La^{3+} cations. (For interpretation of the references to color in this figure legend, the reader is referred to the web version of this article.)

polynomial and a pseudo-Voigt function, respectively. The magnetic susceptibility of $Sr_3NiSb_2O_9$ was measured over the temperature range $5 \leq T/K \leq 300$ using a Quantum Design MPMS 5000 SQUID magnetometer. Data were collected on warming in a field of 100 Oe after cooling the sample both in the absence of an applied field (zero-field cooled, ZFC) and in the measuring field (field cooled, FC). The magnetisation of the sample was measured as a function of applied field at selected temperatures. The sample was cooled from 150 K to the measuring temperature in a field of 50 kOe and data were then collected over the range $-50 \leq H/kOe \leq 50$.

3. Results

Preliminary quantitative analysis of the X-ray diffraction pattern of the product suggested that a monoclinic perovskite phase had formed. The neutron diffraction data were consistent with this conclusion and full, independent analyses of both data sets were therefore undertaken in the space group $P2_1/n$. This space group, which has been used to describe many perovskites in the past [10], allows two different cations to occupy the six-coordinate *B* sites, 2*c* and 2*d*, in an ordered manner. Analysis of both diffraction patterns proceeded smoothly and resulted in the atomic coordinates listed in Tables 1 and 2; the corresponding bond lengths and bond angles derived from the neutron diffraction data are listed in Table 3. The composition of the sample was constrained to be $Sr_3NiSb_2O_9$. In the analysis of the X-ray data the displacement parameters associated with the 2*c* and 2*d* sites were constrained to be equal, as were those of the three crystallographically-distinct oxide ions. The final agreement factors were $R_{wpr}=5.3$ (9.4) %, $\chi^2=4.9$ (3.4) for the neutron (X-ray)-based refinements. The results presented in Table 1 show that one of the two crystallographically distinct six-coordinate sites is largely occupied by antimony whereas the other is occupied by a ~2:1 mixture of nickel and antimony. For reasons that will be discussed below, analyses of the neutron diffraction data were also carried out in selected orthorhombic space groups, including *Pnnm*. The resulting fits were always significantly worse than that obtained in $P2_1/n$ and shown in Fig. 2.

Table 1
Structural parameters of $Sr_3NiSb_2O_9$ derived from X-ray diffraction data collected at 300 K.

Atom	Site	*x*	*y*	*z*	U_{iso} (Å^2)	Occupancy
Sr	4*e*	0.4961(4)	0.4902(2)	0.2503(2)	0.0136(2)	1
Ni/Sb1	2*c*	0	1/2	0	0.0031(1)	Sb: 0.970(2) Ni: 0.030(2)
Ni/Sb2	2*d*	1/2	0	0	0.0031(1)	Sb: 0.363(2) Ni: 0.637(2)
O1	4*e*	0.773(1)	0.766(1)	−0.028(2)	0.009(1)	1
O2	4*e*	0.726(1)	0.271(1)	−0.039(1)	0.009(1)	1
O3	4*e*	0.551(1)	0.001(1)	0.242(1)	0.009(1)	1

Space group $P2_1/n$: $a=5.64381(2)$, $b=5.62299(2)$, $c=7.95687(3)$, $\beta=90.014(2)$.

Table 2
Structural parameters of $Sr_3NiSb_2O_9$ derived from neutron diffraction data collected at 300 K.

Atom	Site	*x*	*y*	*z*	U_{iso} (Å^2)	Occupancy
Sr	4*e*	0.4996(6)	0.4919(6)	0.2496(12)	0.0157(3)	1
Ni/Sb1	2*c*	0	1/2	0	0.002(2)	Sb: 0.971(14) Ni: 0.029(14)
Ni/Sb2	2*d*	1/2	0	0	0.002(2)	Sb: 0.362(14) Ni: 0.638(14)
O1	4*e*	0.7771(8)	0.7749(12)	−0.0288(6)	0.014(1)	1
O2	4*e*	0.7339(9)	0.2656(13)	−0.0225(7)	0.009(1)	1
O3	4*e*	0.5481(4)	0.0033(7)	0.2571(13)	0.0101(5)	1

Space group $P2_1/n$: $a=5.64480(8)$, $b=5.62413(8)$, $c=7.9581(1)$, $\beta=90.010(4)^\circ$.

Table 3
Bond lengths (Å) and bond angles (degrees) in $Sr_3NiSb_2O_9$ derived from neutron diffraction data collected at 300 K.

Ni/Sb1–O1	2.006(6) × 2	Sr–O1	2.831(9)
Ni/Sb1–O2	2.007(6) × 2	Sr–O1	3.146(8)
Ni/Sb1–O3	1.952(10) × 2	Sr–O1	2.789(8)
Ni/Sb2–O1	2.025(5) × 2	Sr–O1	2.531(9)
Ni/Sb2–O2	2.001(6) × 2	Sr–O2	2.839(9)
Ni/Sb2–O3	2.064(10) × 2	Sr–O2	3.058(8)
O1-Ni/Sb1–O2	91.5(4)	Sr–O2	2.619(8)
O1-Ni/Sb1–O3	91.1(2)	Sr–O2	2.764(9)
O2-Ni/Sb1–O3	90.6(2)	Sr–O3	2.762(5)
O1-Ni/Sb2–O2	93.0(4)	Sr–O3	2.890(5)
O1-Ni/Sb2–O3	91.0(2)	Sr–O3	3.093(4)
O2-Ni/Sb2–O3	90.3(2)	Sr–O3	2.554(4)

The temperature dependence of the magnetic susceptibility and the field-dependence of the magnetisation of $Sr_3NiSb_2O_9$ are shown in Figs. 3 and 4, respectively. Fitting the data recorded in the temperature range $150 < T/K < 300$ to the Curie–Weiss law resulted in $\mu_{eff}=3.49(1)$ μ_B per Ni^{2+}, $\theta=-138(1)$ K. The gradient of the curve in Fig. 3 increases on cooling below ~90 K and hysteresis is apparent in this low temperature region. The ZFC susceptibility shows a maximum at 8.7 K whereas the FC susceptibility is essentially constant between 8.7 and 6 K and then increases again between 6 and 2 K. Hysteresis in M(H) is apparent at 2 K, see Fig. 4, with a remanent magnetisation of $\sim 2 \times 10^{-3}$ μ_B per formula unit; no hysteresis is apparent at 7.5 or 15 K.

4. Discussion

Our analysis of the crystal structure of $Sr_3NiSb_2O_9$ shows it to adopt the same monoclinic space group as the other members of